

**Reconstruction of chaotic saddles by classification of unstable periodic orbits:
Kuramoto-Sivashinsky equation**

Yoshitaka Saiki, Michio Yamada, Abraham C.-L. Chian, Rodrigo A. Miranda, and Erico L. Rempel

Citation: *Chaos* **25**, 103123 (2015); doi: 10.1063/1.4933267

View online: <http://dx.doi.org/10.1063/1.4933267>

View Table of Contents: <http://scitation.aip.org/content/aip/journal/chaos/25/10?ver=pdfcov>

Published by the **AIP Publishing**

Articles you may be interested in

[Amplitude modulation for the Swift-Hohenberg and Kuramoto-Sivashinski equations](#)

J. Math. Phys. **55**, 123510 (2014); 10.1063/1.4904486

[Tracking unstable steady states and periodic orbits of oscillatory and chaotic electrochemical systems using delayed feedback control](#)

Chaos **16**, 033109 (2006); 10.1063/1.2219702

[Analysis of chaotic saddles in high-dimensional dynamical systems: The Kuramoto-Sivashinsky equation](#)

Chaos **14**, 545 (2004); 10.1063/1.1759297

[Role of unstable periodic orbits in phase and lag synchronization between coupled chaotic oscillators](#)

Chaos **13**, 309 (2003); 10.1063/1.1518430

[Scale and space localization in the Kuramoto-Sivashinsky equation](#)

Chaos **9**, 452 (1999); 10.1063/1.166419

Cross-pollinate.



Submit your computational article to *CiSE*.

Reconstruction of chaotic saddles by classification of unstable periodic orbits: Kuramoto-Sivashinsky equation

Yoshitaka Saiki,^{1,a)} Michio Yamada,² Abraham C.-L. Chian,³⁻⁷ Rodrigo A. Miranda,⁸ and Erico L. Rempel⁵

¹Graduate School of Commerce and Management, Hitotsubashi University, Tokyo 186-8601, Japan

²Research Institute for Mathematical Sciences (RIMS), Kyoto University, Kyoto 606-8502, Japan

³Paris Observatory, LESIA, CNRS, 92195 Meudon, France

⁴National Institute for Space Research (INPE), P.O. Box 515, São José dos Campos, São Paulo 12227-010, Brazil

⁵Institute of Aeronautical Technology (ITA) and World Institute for Space Environment Research (WISER), São José dos Campos, São Paulo 12228-900, Brazil

⁶School of Mathematical Sciences, University of Adelaide, Adelaide SA 5005, Australia

⁷Department of Biomedical Engineering, George Washington University, Washington, DC 20052, USA

⁸Faculty UnB-Gama, and Plasma Physics Laboratory, Institute of Physics, University of Brasília (UnB), Brasília DF 70910-900, Brazil

(Received 21 July 2015; accepted 1 October 2015; published online 21 October 2015)

The unstable periodic orbits (UPOs) embedded in a chaotic attractor after an attractor merging crisis (MC) are classified into three subsets, and employed to reconstruct chaotic saddles in the Kuramoto-Sivashinsky equation. It is shown that in the post-MC regime, the two chaotic saddles evolved from the two coexisting chaotic attractors before crisis can be reconstructed from the UPOs embedded in the pre-MC chaotic attractors. The reconstruction also involves the detection of the mediating UPO responsible for the crisis, and the UPOs created after crisis that fill the gap regions of the chaotic saddles. We show that the gap UPOs originate from saddle-node, period-doubling, and pitchfork bifurcations inside the periodic windows in the post-MC chaotic region of the bifurcation diagram. The chaotic attractor in the post-MC regime is found to be the closure of gap UPOs. © 2015 AIP Publishing LLC. [<http://dx.doi.org/10.1063/1.4933267>]

Unstable periodic orbits (UPOs) are important fundamental invariant sets which can characterize chaotic invariant sets (chaotic attractor, chaotic saddle). If chaotic saddles are embedded in a chaotic attractor, it is difficult to characterize them, especially in a high dimensional system. In this paper, we study the Kuramoto-Sivashinsky equation, which is a partial differential equation exhibiting chaotic behavior, focusing in the regime after the onset of attractor merging crisis (MC). We detect a large number of UPOs and classify them into three subsets. It is shown that the chaotic saddles in the post-MC regime can be reconstructed by a subset of UPOs (attractor UPOs) originating from the attractor in the pre-MC regime. It is also shown that the post-MC chaotic attractor is characterized by a subset of newly created UPOs (gap UPOs), which fill the gaps between chaotic saddles and reflect the global behavior of the chaotic system generated by the attractor merging crisis.

converge to the chaotic saddle in forward time dynamics; the unstable manifold is the set of points which converge to the chaotic saddle in the backward time dynamics. The chaotic saddle lies on the intersection of its stable and unstable manifolds, which are fractal sets. Thus, their intersection contains gaps along the stable and unstable foliations. Numerically, chaotic saddles can be detected by using several methods such as the sprinkler,^{8,9} the [PIM (Proper Interior Maximum) triple],¹⁰ and the stagger-and-step algorithms.¹¹

Large-scale invariant sets such as chaotic attractors can undergo bifurcations as a control parameter is varied. These bifurcations include the sudden disappearance or sudden changes in the size and/or type of the set.¹²⁻¹⁶ An attractor MC is an example of global bifurcation in which two or more chaotic attractors merge to form one single chaotic attractor.¹⁷ At MC, chaotic attractors simultaneously touch the boundary separating their basins of attraction and collide with one or more UPOs on the basin boundary. Although most previous works on MC were restricted to low-dimensional dynamical systems, there are some works on MC of high-dimensional systems. Platt *et al.*¹⁸ investigated a two-dimensional Kolmogorov flow governed by the incompressible Navier-Stokes equations with a steady, spatially periodic forcing and found the occurrence of a MC. Kobayashi and Mizuguchi¹⁹ studied a MC in a one-dimensional parametrically forced complex Ginzburg-Landau equation. Rempel and Chian²⁰ presented a characterization of a MC in the Kuramoto-Sivashinsky equation by demonstrating the collision of two chaotic attractors with a mediating UPO on the boundary of their basins of attraction. In addition, they

I. INTRODUCTION

Chaotic saddles are nonattracting chaotic sets responsible for nonlinear phenomena such as chaotic transients, chaotic scattering, and fractal basin boundaries.¹⁻⁸ A chaotic saddle is characterized by its associated stable and unstable manifolds. The stable manifold is the set of points which

^{a)}yoshi.saiki@r.hit-u.ac.jp

showed the existence of chaotic saddles in the post-MC regime. Szabó *et al.*^{21,22} argued with some examples of map systems that the gaps of chaotic saddles become densely filled in an interior crisis due to the appearance of gap UPOs with extremely long periods.

In this paper, we focus on the detection and classification of UPOs embedded in a chaotic attractor in the post-MC regime, and the reconstruction of chaotic saddles using a subset of these UPOs in the Kuramoto-Sivashinsky equation (KSE). UPOs in the KSE have been studied in a series of works.^{20,23–32} For example, Christiansen *et al.*²³ reported that the cycle expansion theory can be applied to compute global averages of attracting and nonattracting chaotic sets of the KSE with periodic boundary conditions; Zoldi and Greenside²⁴ investigated the statistical error associated with estimations of the fractal dimension of a spatiotemporally chaotic attractor as a function of the number of known UPOs of the KSE with rigid boundary conditions. Lan and Cvitanović²⁷ studied UPOs in the KSE with periodic boundary conditions in the same setting as Christiansen *et al.*,²³ but in a turbulent regime. They showed that the UPOs can be organized into trinary symbolic dynamics in this regime. They also studied the relative periodic orbits appearing in the turbulent regime, which we will call gap unstable periodic orbits. The present work focuses on the bifurcations of the UPOs near the MC occurring at the parameters between two regimes studied by Christiansen *et al.*²³ and Lan and Cvitanović.²⁷ We confirm agreements between the chaotic saddles identified by the PIM triple method and those identified by a set of UPOs classified by the bifurcation analysis, and clarify the roles of three types of UPOs in the post-MC regime. This paper is organized as follows. In Section II, we discuss the numerical setting to study the KSE and obtained the bifurcation diagram for attractors and chaotic saddles. In Section III, we detect a large number of UPOs and classify them into three subsets based on their origins. In Section IV, chaotic saddles are reconstructed by using a subset of UPOs, and it is shown that gaps in chaotic saddles are filled with another set of UPOs. We conclude our remarks in Section V.

II. BIFURCATION DIAGRAM FOR ATTRACTORS AND CHAOTIC SADDLES

The Kuramoto-Sivashinsky equation can be written as

$$u_t = -u_{xx} - \nu u_{xxx} - (u^2)_x, \tag{1}$$

where ν is a “viscosity” control parameter. We assume periodic boundary conditions $u(x, t) = u(x + 2\pi, t)$, following Refs. 23 and 20. By employing the Galerkin method, we apply a Fourier decomposition to the function $u(x, t) = \sum_{k=-\infty}^{\infty} b_k(t)e^{ikx}$ and obtain

$$\dot{b}_k = (k^2 - \nu k^4)b_k - ik \sum_{m=-\infty}^{\infty} b_m b_{k-m}, \quad k = -\infty, \dots, +\infty, \tag{2}$$

where the coefficients b_k are complex variables. We simplify the system by assuming that b_k are purely imaginary, $b_k = -ia_k/2$, where a_k are real, and obtain

$$\dot{a}_k = (k^2 - \nu k^4)a_k - \frac{k}{2} \sum_{m=-\infty}^{\infty} a_m a_{k-m}, \quad k = -\infty, \dots, +\infty. \tag{3}$$

This simplification corresponds to choosing reflection-invariant modes of the system, which represent the subspace of odd functions, $u(x, t) = -u(-x, t)$, and the solutions stay in this invariant subspace for all time. This breaks the continuous shift symmetry of the system, and only discrete shifts by π are allowed. See Ref. 28 for the detailed discussions of the symmetries of the system. This equation contains unnecessary components. Since $u(x, t)$ is real, $-ia_k = ia_{-k}$, and it is not necessary to compute the modes with negative k . Moreover, $a_k = 0$ for $|k| > N$, and some operations in the nonlinear term can be dropped. Thus, the simplified equations can be written in the truncated form

$$\begin{aligned} \dot{a}_k &= (k^2 - \nu k^4)a_k \\ &+ \frac{k}{2} \left(\sum_{m=k-N}^{-1} a_{-m} a_{k-m} - \sum_{m=1}^{k-1} a_m a_{k-m} + \sum_{m=k+1}^N a_m a_{m-k} \right), \\ &k = 1, \dots, N. \end{aligned} \tag{4}$$

We solve Eq. (4) with $N = 16$.

Fig. 1(a) displays a superposition of bifurcation diagrams at the Poincaré section defined by $a_1 = 0$ and $\dot{a}_1 > 0$,

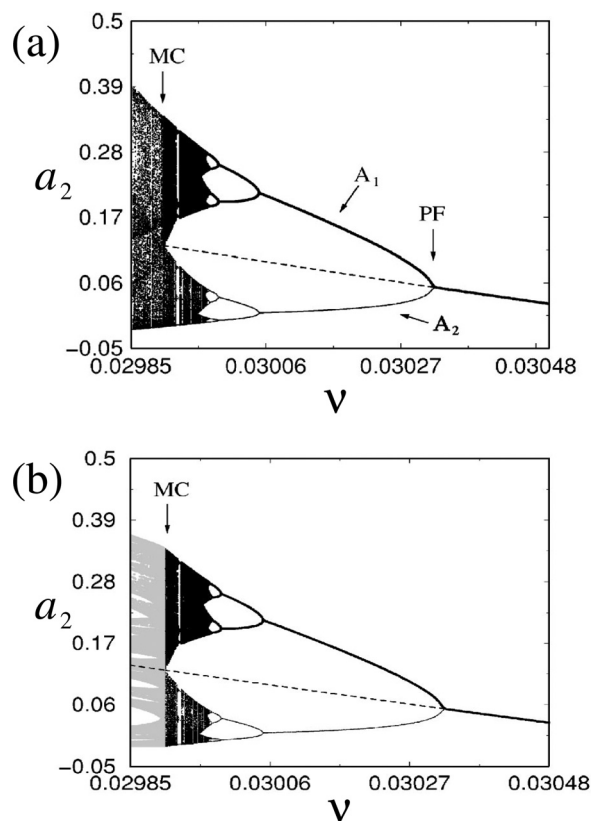


FIG. 1. (a) Superposition of bifurcation diagrams for attractors A_1 and A_2 (black), showing the merging of the two attractors into a single attractor at MC. The dashed line represents the p-1 m-UPO. (b) Conversion of attractors A_1 and A_2 into two chaotic saddles CS_1 and CS_2 (gray) after MC, respectively. The two chaotic saddles, computed by the PIM-triple method, are separated by the m-UPO.

for two attractors (A_1 and A_2), showing their merging into a single attractor at MC, where $\nu_{MC} \approx 0.02990$. The dashed line represents an UPO created at the pitchfork bifurcation indicated by PF. This UPO is named a mediating UPO (m-UPO) because it mediates the MC. The symmetry between A_1 and A_2 reflects an invariance of Eq. (4) under the shift $u(x, t) \rightarrow u(x + \pi, t)$, which is a particular case of the translation invariance property of the system. After colliding with the m-UPO, the two pre-crisis chaotic attractors lose their stability and are converted into two chaotic saddles (CS_1 and CS_2) immersed in the merged chaotic attractor.²⁰ In Fig. 1(b), we plot the same bifurcation diagram of Fig. 1(a) (black) up to MC ($\nu > \nu_{MC}$), and after MC ($\nu < \nu_{MC}$), we plot the Poincaré points of the two chaotic saddles (gray). The white spaces within the gray areas are gaps that reflect the discontinuous and fractal structure of the chaotic saddles. The two chaotic saddles CS_1 and CS_2 are separated by the period-1 (p-1) m-UPO (dashed line) in Fig. 1(b). Here, period n (p- n) denotes the period of a given UPO in the Poincaré map. In the full 15-D Poincaré map, the stable manifold of the m-UPO separates the post-crisis chaotic saddles. The same manifold forms the basin boundary of the two pre-MC chaotic attractors.

III. CLASSIFICATION OF UNSTABLE PERIODIC ORBITS

We focus our attention first in the regions nearby $\nu = \nu_{MC}$ by detecting 537 UPOs of periods up to 11 numerically at $\nu = 0.02987$ ($\nu < \nu_{MC}$) using the Newton-Raphson-Mees method.³⁴ Next, we increase the control parameter value to $\nu = 0.02991$ ($\nu > \nu_{MC}$) and follow the evolution of these UPOs across the MC point. The post-MC UPOs can be classified into three subsets: (1) a-UPO (attractor UPO) which exists in both pre-MC ($> \nu_{MC}$) and post-MC ($< \nu_{MC}$) regimes, (2) g-UPO (gap UPO) which exists only in the post-MC ($< \nu_{MC}$) regime, and (3) the m-UPO (mediating UPO) which is located on the boundary of the basins of attraction of the two coexisting chaotic attractors in the pre-MC regime. Note that our notation “a-UPO” may sound awkward when expanded as “attractor-unstable periodic orbit.” Nevertheless, we chose this term for simplicity, and it refers to the UPOs embedded in chaotic attractors that exist prior to the attractor merging crisis.

Fig. 2 shows three subsets of examples of UPOs found at $\nu = 0.02987$ ($\nu < \nu_{MC}$), and traced until $\nu = 0.02991$ ($\nu > \nu_{MC}$). For simplicity, we plot only one branch of each UPO. This figure shows that p-7, p-8, and p-9 g-UPOs (green) exist only in the post-MC regime, whereas p-2, p-3, and p-4 a-UPOs (red) and p-1 m-UPO (black) exist in both post- and pre-MC regimes.

We exemplify the appearance of some g-UPOs by focusing on a periodic window in the post-MC regime. Fig. 3(a) shows a detailed view of the bifurcation diagram after the attractor merging crisis. Fig. 3(b) shows an enlargement of one branch of the p-7 periodic window indicated by an arrow in Fig. 3(a), superposed by three examples of gap UPOs created within this periodic window. The green line represents, respectively: (1) a p-7 g-UPO_{SN} originating from

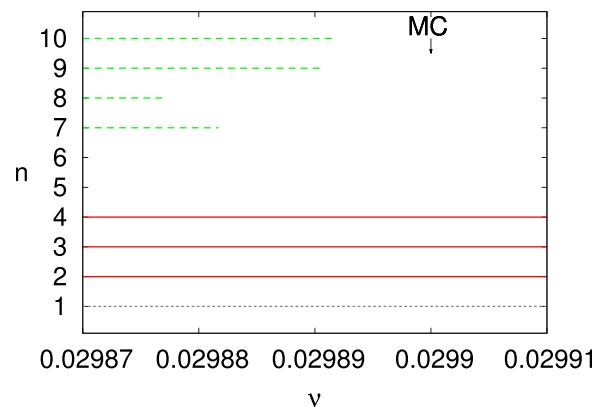


FIG. 2. Branches of three subsets of examples of UPOs of period n ($p - n$) by changing ν near MC indicated by arrow. The first subset are g-UPOs (green dashed line) of p-7, p-8, p-9, and p-10. The second are a-UPOs (red line) of p-2, p-3, and p-4. The third is m-UPO (black dotted line) of p-1. The g-UPOs detected at $\nu = 0.02987$ exist only in the post-MC regime, whereas the a-UPOs and the m-UPO exist in both pre- and post-MC regimes.

a saddle-node bifurcation (SN) which marks the beginning of this periodic window; (2) a p-7 g-UPO_{PF} evolved from a PF which mediates a MC within this periodic window; (3) a p-7 g-UPO_{PD} produced by the first period-doubling bifurcation (PD).

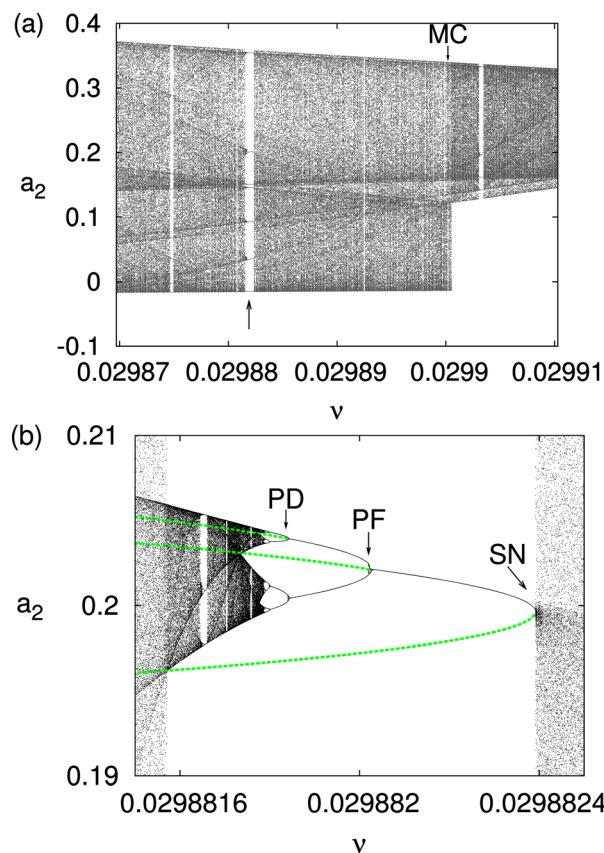


FIG. 3. (a) Detailed view of the bifurcation diagram in the post-MC regime, showing a p-7 periodic window indicated by an arrow. (b) Enlargement of one branch of the p-7 periodic window and its symmetric attractor superposed by p-7 g-UPO_{SN}, p-7 g-UPO_{PF}, and p-7 g-UPO_{PD}. The UPOs are marked green. At the PF point two symmetric periodic attractors are created (upper and lower branches separated by the green dotted line in the bifurcation diagram).

Fig. 4 shows the projections of the phase-space trajectories of UPOs of each subset projected on the (a_1, a_2) plane detected at $\nu = 0.02987$; (a) p-1 m-UPO, (b) p-4 a-UPO, (c) p-7 g-UPO_{SN}, (d) p-7 g-UPO_{PF}, (e) p-7 g-UPO_{PD}, and (f) p-8 g-UPO. This figure shows that in these projections, the m-UPO (Fig. 4(a)) and the g-UPOs (Figs. 4(c)–4(f)) display “symmetric” shapes, whereas the a-UPO (Fig. 4(b)) displays an “asymmetric” shape. Note that g-UPOs look “symmetric,” but most are not self-dual exactly under half domain shift symmetry of the orbits. In fact, it is easily seen that g-UPO in Figs. 4(e) and 4(f) are not self-dual, although g-UPOs in Figs. 4(c) and 4(d) are self-dual.

Fig. 5 shows the Poincaré plots of the two chaotic saddles CS_1 and CS_2 (gray) embedded in the post-MC chaotic attractor, superposed by the p-7 g-UPO_{SN} (Fig. 5(a)), the p-7 g-UPO_{PF} (Fig. 5(b)), and the p-7 g-UPO_{PD} (Fig. 5(c)). This figure clearly shows that the g-UPOs are located within the gaps of the two chaotic saddles.

IV. RECONSTRUCTION OF CHAOTIC SADDLES

Since the chaotic saddles embedded in the post-MC chaotic attractor exhibit fractal structure along the unstable foliation, with zero Lebesgue measure, they have been called by Szabó and Tél,³³ the “geometrical backbone” of the chaotic attractor. The g-UPOs, on the other hand, fill in the gaps

along the unstable foliation of the chaotic saddles, being called the “bulk” of the chaotic attractor.^{22,33} Since the g-UPOs are densely embedded within the chaotic attractor, and the a-UPOs are densely embedded within the chaotic saddle, we naturally expect that the g-UPOs should resemble the chaotic attractor, and the a-UPOs should resemble the fractal structure of the two chaotic saddles. In order to reconstruct the chaotic saddles embedded in the post-MC chaotic attractor, evolved from the pre-MC chaotic attractors, we first detect UPOs for a fixed post-crisis value of ν and then classify them following the aforementioned procedure. Fig. 6 shows the Poincaré plots of the detected p-8 g-UPOs (Fig. 6(a)), p-9 g-UPOs (Fig. 6(b)) and p-10 g-UPOs (Fig. 6(c)) at $\nu = 0.02987$. It can be seen that the sets of g-UPOs with higher periods tend to fill smaller gaps. This is consistent with the fact that, in the post-MC regime close to the transition point, gaps are very small and are filled with g-UPOs with extremely long periods. The lowest periods of the Poincaré map of detected g-UPOs are 6, 7, and 9 for $\nu = 0.02986$, 0.02987, and 0.02989, respectively, which means that the lowest periods of the created g-UPOs are relatively long in the post-MC regime, close to ν_{MC} (~ 0.02990), but become shorter as ν moves away from ν_{MC} . We can confirm this result from Table I, which shows the number of detected UPOs of each subset at $\nu = 0.02987$ away from ν_{MC}

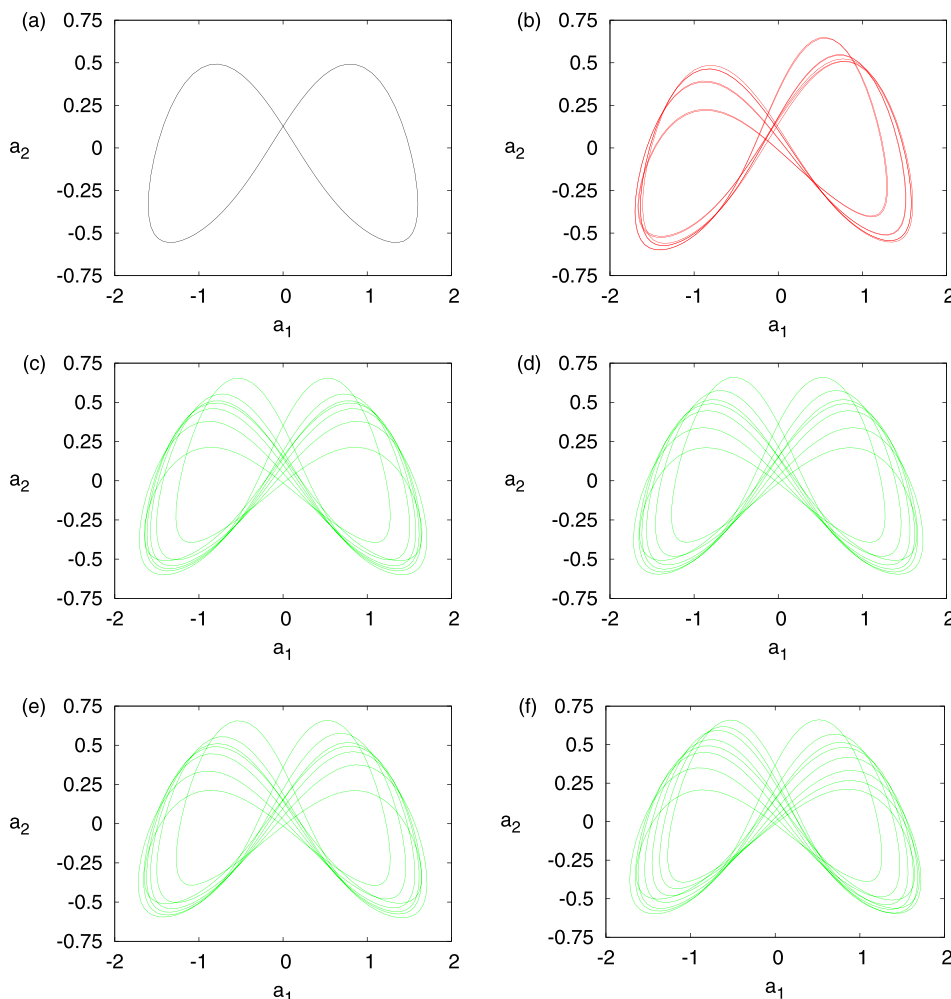


FIG. 4. Projection onto the (a_1, a_2) plane of: (a) p-1 m-UPO, (b) p-4 a-UPO, (c) p-7 g-UPO_{SN}, (d) p-7 g-UPO_{PF}, (e) p-7 g-UPO_{PD}, and (f) p-8 g-UPO for $\nu = 0.02987$, which is the starting point of Fig. 3(a). (c)–(e) correspond to the three branches in Fig. 3(b).

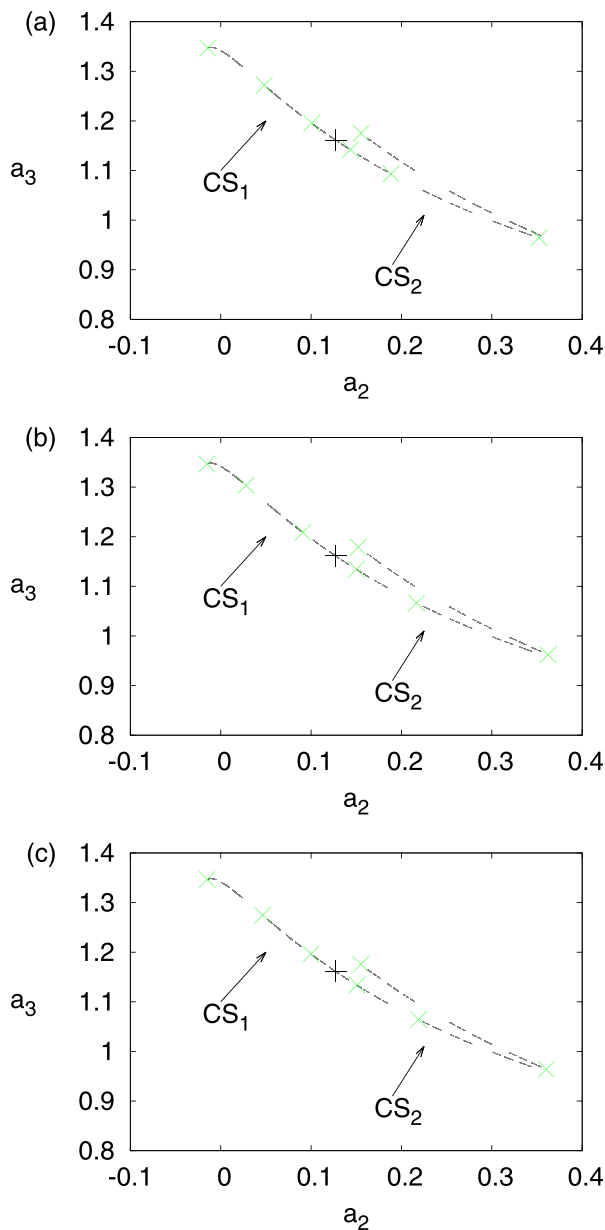


FIG. 5. Poincaré plots on the (a_2, a_3) plane at $\nu = 0.02987$ of chaotic saddles (gray) CS_1 and CS_2 computed by the PIM-triple method, superposed by a respective gap UPO (green crosses) (a) p-7 g-UPO_{SN}, (b) p-7 g-UPO_{PF}, and (c) p-7 g-UPO_{PD}. The p-1 m-UPO is denoted by a black cross. CS_1 is the gray dots to the left of the black cross, and CS_2 is the gray dots to the right of the black cross, as indicated by the arrows.

and 0.02989 closer to ν_{MC} . Our result is consistent with the finding of Szabó *et al.*^{21,22} for an interior crisis of map systems, and can explain the widening of gaps within chaotic saddles with decreasing ν observed in Fig. 1(b). Since near the merging crisis the gap sizes tend to zero, the period of the existing g-UPOs tend to infinity, which is consistent with the values in Table I, where the lowest period g-UPOs have longer periods as the parameter approaches the MC point.

Now, we direct our attention to the reconstruction of the two chaotic saddles evolved from the two pre-MC chaotic attractors using the classified UPOs. Figures 7(a) and 7(b) show the Poincaré plots of the post-MC chaotic attractor and

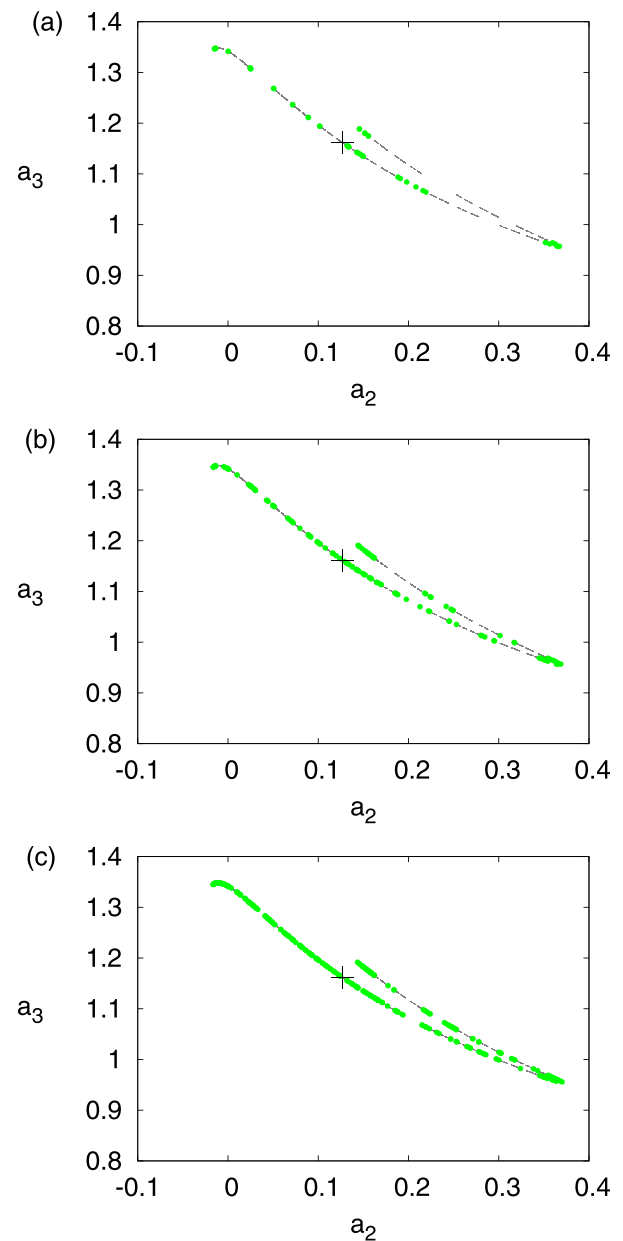


FIG. 6. Poincaré plots on the (a_2, a_3) plane at $\nu = 0.02987$ of chaotic saddles (gray) CS_1 and CS_2 computed by the PIM-triple method superposed by a subset of g-UPOs (green points): (a) p-8 g-UPOs, (b) p-9 g-UPOs, and (c) p-10 g-UPOs; the p-1 m-UPO is denoted by a black cross.

the two embedded chaotic saddles (CS_1 and CS_2), respectively, at $\nu = 0.02987$. The two chaotic saddles CS_1 and CS_2 were computed using the PIM triple method.^{10,20} Figs. 7(c) and 7(d) show the Poincaré plots of a set of g-UPOs and a set of a-UPOs, respectively. From this figure, it can be confirmed that the bulk of the chaotic attractor (Fig. 7(a)) is formed by the g-UPOs (Fig. 7(c)), whereas the chaotic saddles CS_1 and CS_2 (Fig. 7(b)) are reconstructed from the a-UPOs (Fig. 7(d)). Figures 7(b) and 7(c) also show that the gaps within chaotic saddles are filled with g-UPOs. Note that each a-UPO is located in either one of the two regions separated by the m-UPO, whereas each g-UPO has Poincaré points located in both regions. It should be remarked that in the post-MC regime the chaotic attractor (Fig. 7(a)) is considered to be the closure of the set of all gap UPOs (*cf.* Fig. 7(c)).

TABLE I. Total number of m-UPOs, a-UPOs, and g-UPOs and the ratio of g-UPOs detected for $\nu = 0.02987$ (away from ν_{MC}) and 0.02989 (closer to ν_{MC}) in the post-MC regime. Near ν_{MC} , only g-UPOs with long periods are observed. The number of UPOs includes their symmetry copies.

Away from ν_{MC} ($\nu = 0.02987$)										
Period	1	2	3	4	5	6	7	8	9	10
#total	1	2	4	4	12	14	37	72	105	172
#m-UPO	1	0	0	0	0	0	0	0	0	0
#a-UPO	0	2	4	4	12	14	32	60	74	110
#g-UPO	0	0	0	0	0	0	5	12	31	62
g-UPO ratio	0.00	0.00	0.00	0.00	0.00	0.00	0.14	0.17	0.30	0.36
Closer to ν_{MC} ($\nu = 0.02989$)										
Period	1	2	3	4	5	6	7	8	9	10
#total	1	2	4	4	16	14	32	66	124	184
#m-UPO	1	0	0	0	0	0	0	0	0	0
#a-UPO	0	2	4	4	16	14	32	66	118	170
#g-UPO	0	0	0	0	0	0	0	0	4	14
g-UPO ratio	0.00	0.00	0.00	0.00	0.00	0.00	0.00	0.00	0.03	0.08

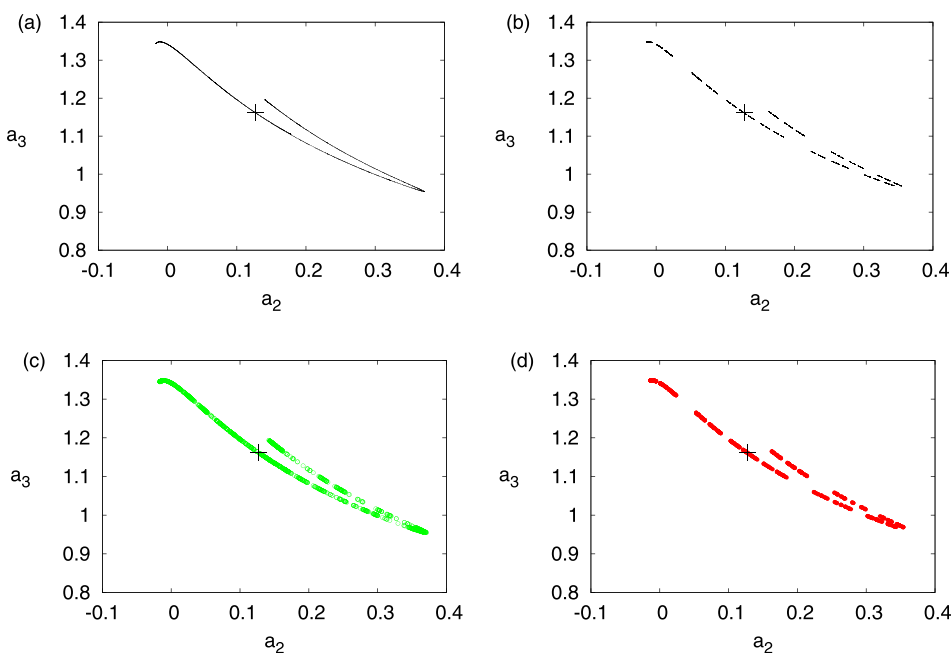


FIG. 7. Poincaré plots on the (a_2, a_3) plane at $\nu = 0.02987$: (a) the post-MC chaotic attractor, (b) chaotic saddles CS_1 and CS_2 computed by the PIM-triple method, (c) g-UPOs, and (d) chaotic saddles reconstructed by a subset of a-UPOs. The p-1 m-UPO is denoted by a black cross.

V. CONCLUSION

We identified a large number of UPOs numerically obtained from the Kuramoto-Sivashinsky equation in the post-MC regime after an attractor MC occurs. The UPOs are traced by changing a control parameter and classified into three subsets: (1) attractor UPO, which exists in the chaotic attractor(s) in both pre-MC and post-MC regimes, (2) gap UPO, which exists only in post-MC, and (3) mediating UPO, which is located on the boundary of the basins of attraction of the two pre-MC chaotic attractors. We showed that gap UPOs are created via saddle-node, period-doubling, and pitchfork bifurcations associated with the post-MC periodic windows. We demonstrated that the two chaotic saddles evolved from the MC can be reconstructed from the attractor UPOs embedded in two coexisting attractors prior to the attractor MC, and that their gaps are filled

with gap UPOs which connect two chaotic saddles separated by the mediating UPO and its stable manifold. The chaotic attractor in the post-MC regime can be characterized by a set of gap UPOs.

ACKNOWLEDGMENTS

The authors would like to thank referees for their helpful comments and suggestions to improve our manuscript. This work was supported by KAKENHI (26610034, 23740065, 15K13458, 24340016, and 22654014), an incentive system for young researchers of the Academic Center for Computing and Media Studies at Kyoto University, and Brazilian agencies CNPq, CAPES (88881.068051/2014-01) and FAPESP (2013/22314-7). Y.S. and A.C.L.C. are grateful to the kind hospitality of RIMS, Kyoto University and Paris Observatory. A.C.L.C. acknowledges the award of a Marie

Curie International Incoming Fellowship and a Fulbright-CAPEF Fellowship, and the kind hospitality of UoA and GWU.

- ¹A. C.-L. Chian, R. A. Miranda, E. L. Rempel, Y. Saiki, and M. Yamada, *Phys. Rev. Lett.* **104**, 254102 (2010).
- ²P. R. Muñoz, J. J. Barroso, A. C.-L. Chian, and E. L. Rempel, *Chaos* **22**, 033120 (2012).
- ³R. A. Miranda, E. L. Rempel, A. C.-L. Chian, N. Seehafer, B. A. Toledo, and P. R. Muñoz, *Chaos* **23**, 033107 (2013).
- ⁴A. C.-L. Chian, P. R. Muñoz, and E. L. Rempel, *Phys. Rev. E* **88**, 052910 (2013).
- ⁵E. Ott, *Chaos in Dynamical Systems*, 2nd ed. (Cambridge University Press, Cambridge, 2002).
- ⁶Y.-C. Lai and T. Tél, *Transient Chaos* (Springer, 2011).
- ⁷T. Tél and Y.-C. Lai, *Phys. Rep.* **460**, 245 (2008).
- ⁸H. Kantz and P. Grassberger, *Physica D* **17**, 75 (1985).
- ⁹G.-H. Hsu, E. Ott, and C. Grebogi, *Phys. Lett. A* **127**, 199 (1988).
- ¹⁰H. E. Nusse and J. A. Yorke, *Physica D* **36**, 137 (1989).
- ¹¹D. Sweet, H. E. Nusse, and J. A. Yorke, *Phys. Rev. Lett.* **86**, 2261 (2001).
- ¹²K. T. Alligood, E. Sander, and J. A. Yorke, *Ergodic Theory Dyn. Syst.* **22**(4), 953–972 (2002).
- ¹³K. T. Alligood, E. Sander, and J. A. Yorke, *Phys. Rev. Lett.* **96**, 244103 (2006).
- ¹⁴K. T. Alligood, E. Sander, and J. A. Yorke, *Rend. Semin. Mat. Univ. Politecnico Torino* **65**(1), 1–15 (2007).
- ¹⁵C. Robert, K. T. Alligood, E. Ott, and J. A. Yorke, *Physica D* **144**, 44–61 (2000).
- ¹⁶E. Sander and J. A. Yorke, *Ergodic Theory Dyn. Syst.* **29**, 715–731 (2009).
- ¹⁷C. Grebogi, E. Ott, F. Romeiras, and J. A. Yorke, *Phys. Rev. A* **36**, 5365 (1987).
- ¹⁸N. Platt, L. Sirovich, and N. Fitzmaurice, *Phys. Fluids A* **3**, 681–696 (1991).
- ¹⁹M. U. Kobayashi and T. Mizuguchi, *Phys. Rev. E* **73**, 016212 (2006).
- ²⁰E. L. Rempel and A. C.-L. Chian, *Phys. Rev. E* **71**, 016203 (2005).
- ²¹K. G. Szabó, Y.-C. Lai, T. Tél, and C. Grebogi, *Phys. Rev. Lett.* **77**, 3102–3105 (1996).
- ²²K. G. Szabó, Y.-C. Lai, T. Tél, and C. Grebogi, *Phys. Rev. E* **61**, 5019–5032 (2000).
- ²³F. Christiansen, P. Cvitanović, and V. Putkaradze, *Nonlinearity* **10**, 55–70 (1997).
- ²⁴S. M. Zoldi and H. S. Greenside, *Phys. Rev. E* **57**(3), R2511 (1998).
- ²⁵A. C.-L. Chian, E. L. Rempel, E. E. Macau, R. R. Rosa, and F. Christiansen, *Phys. Rev. E* **65**, 035203 (2002).
- ²⁶Y. Lan and P. Cvitanović, *Phys. Rev. E* **69**, 016217 (2004).
- ²⁷Y. Lan and P. Cvitanović, *Phys. Rev. E* **78**, 026208 (2008).
- ²⁸P. Cvitanović, R. L. Davidchack, and E. Siminos, *SIAM J. Appl. Dyn. Syst.* **9**, 1–33 (2010).
- ²⁹E. L. Rempel, A. C.-L. Chian, E. E. N. Macau, and R. R. Rosa, *Chaos* **14**, 545–556 (2004).
- ³⁰E. L. Rempel, A. C.-L. Chian, A. J. Preto, and S. Stephany, *Nonlinear Processes Geophys.* **11**, 691–700 (2004).
- ³¹Y. Morita, N. Fujiwara, M. U. Kobayashi, and T. Mizuguchi, *Chaos* **20**, 013126 (2010).
- ³²Y. Saiki and M. Yamada, in *Nankai Series in Pure, Applied Mathematics and Theoretical Physics*, edited by H. Chen, Y. Long, and Y. Nishiura (World Scientific, 2013), Vol. 10, pp. 145–154.
- ³³K. G. Szabó and T. Tél, *Phys. Lett. A* **196**, 173–180 (1994).
- ³⁴J. H. Curry, in *Global Theory of Dynamical Systems*, edited by Z. Nitecki and C. Robinson (Springer-Verlag, Berlin, 1979), pp. 111–120.